HAL open science

Accurate absorption spectroscopy of water vapor near 1.64 μm in support of the MEthane Remote LIdar missioN (MERLIN)

S. Vasilchenko, H. Tran, D. Mondelain, S. Kassi, A. Campargue

▶ **To cite this version:**

S. Vasilchenko, H. Tran, D. Mondelain, S. Kassi, A. Campargue. Accurate absorption spectroscopy of water vapor near 1.64 μm in support of the MEthane Remote LIdar missioN (MERLIN). Journal of Quantitative Spectroscopy and Radiative Transfer, 2019, 235, pp.332-342. 10.1016/j.jqsrt.2019.06.027 . hal-02345499

HAL Id: hal-02345499

https://hal.sorbonne-universite.fr/hal-02345499v1

Submitted on 20 Dec 2021

HAL is a multi-disciplinary open access archive for the deposit and dissemination of scientific research documents, whether they are published or not. The documents may come from teaching and research institutions in France or abroad, or from public or private research centers.

L'archive ouverte pluridisciplinaire **HAL**, est destinée au dépôt et à la diffusion de documents scientifiques de niveau recherche, publiés ou non, émanant des établissements d'enseignement et de recherche français ou étrangers, des laboratoires publics ou privés.

Distributed under a Creative Commons Attribution - NonCommercial 4.0 International License

Version of Record: https://www.sciencedirect.com/science/article/pii/S0022407319301669
Manuscript_66b2194ad683e022d360047f5e90a972

The influence of hole networks on the adsorption-induced frequency shift of a perforated nanobeam using non-local elasticity theory

Hicham Bourouina,[a, b] Réda Yahiaoui,[b] Rachid Kerid,[c] Kamal Ghoumid,[d] Isabelle Lajoie,[b] Fabien Picaud [b] and Guillaume Herlem[b]

[a] *Physics Laboratory, Normal School of Bou-Saada, M'Sila28200, Algeria*
[b] *Nanomedicine Lab, University of Franche-Comte, Besancon 25000, France*
[c] *Electronics Institute, University of Blida, BP. 270 09000, Algeria*
[d] *EIT Department, ENSAO, Mohamed First University, Oujda , Morocco*

E-mail: hi.bourouina@gmail.com
reda.yahiaoui@univ-fcomte.fr

Abstract: Modelling the non-local frequency shift caused by the adsorption phenomenon of an adatom-perforated nanobeam system taking into account the influence of shear distortion as well as small-scale behavior has been proposed in this paper. The nanobeam structure is a one-dimensional system perforated with a network of periodic square holes. The small-scale behavior was modelled using the elasticity theory of Eringen, while the explicit shear force and bending moment were determined from the standard dynamic equations. Adatom-adatom energy and adatom-substrate energy were introduced using the van der Waals (vdW) interactions in the framework of Lennard-Jones (6-12) potential to determine the total shift in energy. Both the shear beam model (SBM) and Euler beam model (EBM) were derived in this work by modifying the system coupled equations. The frequency shift for the *H/Au(100)* system was calculated, which showed that its observed value depends on the size and number of holes as well as the mode number and adsorption density. These results have been interpreted in detail toward the appropriate design of mass detection devices.

1. Introduction

Adatom-nanobeam systems have been extensively employed in nanotechnology as mechanical devices with low costand reduced size for mass detection applications. Due to their advantages, such as enhanced reliability [1], fast response ability [2] and high sensitivity, these interesting systems have attracted a significant amount of attention and have been an active part of nanotechnology research. These systems have various applications in the microengineering field, such as micromechanics and biomechanics. In particular, micro/nanoscale systems including carbon nanotubes (CNTs) [3] and ZnO nanowires have been used as building blocks for many microelectromechanical systems (MEMS) and nanoelectromechanical systems (NEMS). Nanostructures have also been fabricated based on homogeneous materials, such as functionally graded (FG) nanobeams, to improve the dynamic behavior of these microsystems [4–6]. For instance, several various dynamic behavior approaches have been developed to estimate the interaction energy [7–8] and frequency shift upon the adsorption of atomic or molecular species [9–11] observed experimentally. Chen *et* al.[12] determined the local shift induced by chemical elements on a beam structure with micrometric dimensions. By accounting for the increase in the number of nanoparticles and variation in the microelastic constant due to the adsorbed adatoms, Cherian et al. [13] attributed the local change to the contribution of these two properties. In addition, Hagan et al. [14] evaluated the change in microdeformation caused by DNA added onto the surface of the structures. Moreover, Wang et al. [15] studied the physical properties of thin monolayers of silicon-based nanoresonators. They included the influence of the active layer formed after the treatment of the nanostructure and gas adsorption. Kim et al. [16] determined both the separation and speciation of a mixture for various explosives on the picogram level by calculating the shift in deformation of the nanostructure. In a noticeable contribution, Huber et al. [17] studied RNA using a microcantilever and investigated the BRAF gene using a nanomechanical system. Sage et al. [18] investigated the mass spectra obtained from the analytes using NEMS-MS and showed that the analyses were insensitive to the charge state. Note that several other works dealing with adatom or molecular detection devices have been achieved recently. They have demonstrated that the change in the permittivity of a resonator constructed from carbon nanotubes can be used as an excellent parameter to detect molecular species or differentiate between the enantiomers of the same chiral molecule [19–21].

Inspired by the great potential of adatom-nanobeam systems, many theoretical and experimental approaches have been conducted to gain insight into the adatom-nanobeam interactions, mostly modelled using van der Waals (vdW) interactions. Because of its scientific and strategic potential, the mechanical behavior of nanobeams has been investigated by scientists and engineers in advanced studies dedicated to materials and structures. This aims to gain an understanding of the dynamic analysis of nanostructures for the precise prognosis of motion characteristics [23–25], where various analytical, semi-analytical and numerical models have been used to investigate the dynamic behavior of nanobeams. Numerous experimental observations using dynamic control of the structural behavior have concluded that the added mass coming from both chemical [13–14 , 16, 18] and biological [14, 17] mixtures yields a vibration frequency shift attributed to the variation inthe equivalent mass by the

© 2019 published by Elsevier. This manuscript is made available under the CC BY NC user license
https://creativecommons.org/licenses/by-nc/4.0/

adatoms distributed on the supported systems. These nanostructures are stable by nature. They are held up by the supports to form a stable structure without any degree of indeterminacy. Depending on the applied load, these nanostructures undergo bending and shearing. Zhang et al.[10] proposed a local frequency shift model combining the standard material elasticity and Euler beam theory. They deduced the bending stiffness in the dynamic vibration of the adatom-microbeam system and the total elastic strain energy including the vdW interaction energy. Using a similar technique based on the nanobeam theory of Timoshenko, Gheshlaghi et al. [11] determined another local shift model, which covers the influence of shear and bending. The authors generalized their approach by analyzing the local shift depending on the density and dimensions.

However, determining the local frequency does not predict the influence of non-local behavior using the standard elasticity where practical verifications indicatesize-dependent nanobeam behavior [26, 27]. Non-local behavior has been investigated using various material models such as the shear deformation model, stress-driven model and non-local material model. These approaches take into consideration the influence of the screen introducing intrinsic effects [28]. In addition, several non-local contributions have been proposed using astress-driven model for elastic nanobeams andstress-driven mixture model for nanobeams, as well as axisymmetric nanoplates. The non-local parameter translates the influence of small scale behavior on the mechanical properties. According to Eringen's non-local material model, this parameter is appropriate to the materials structure and can be determined from lattice dynamics simulations using non-local theoretical results.

Many studies have used scale-dependent theories to account for the non-local behavior observed in Eringen's non-local theory of materials [29] to model the influence of the initial edge displacement observed during electrical and magnetic instabilities [30]. Farajpour et al. modeled the non-linear behavior of buckling analysis for magneto-electro-elastic CNT-MT hybrid shells usingnon-local continuum mechanics [31]. The numerical results of this work indicated that non-linear buckling loads are highly sensitive to the non-local parameter and that the non-dimensional buckling load decreases with the electric voltage. Li et al. [32] investigated the non-local response analysis of the thermo-electro-mechanical behavior ofmulti-layered piezoelectric plates with nanometric dimensions and various boundary conditions. Some authors have found that the nanoplate dimensions change with temperature and other physical parameters can be exploited to adapt the induced frequency. Other studies have used non-local continuum theory to model the surface effects on the buckling analysis of microtubules based on first-order shear deformation theory [33] and to determine the frequency response of microsensors under non-uniform preload conditions [34]. In addition, both the size-dependent diffusion-elasticity on shock for electrochemical components at various concentrations [35] and vibrations of initially stressed CNT under magneto-thermal environment [36] have been investigated.

Non-local theory of material elasticity established by Eringen is based on the assumption that stress at a point in the structure is related to the strain at all points in which constitutive theory reports the total force between the length scale and the atoms [28]. In this theory, both the dispersion waves and wave propagation in the material can be studied using non-local constitutive equations. The non-local parameter is proposed as an appropriate description for the nanostructure, which can be determined using lattice dynamics theory andnon-local elasticity theory [37]. The shift in the frequency can be considered as an indicator to evaluate the non-local dynamic behavior in the nanostructure. Non-local behavior on micrometric dimensions makes the vibrated systems more flexible and non-local material theory can be used to make more predictions at higher frequencies [28]. Based on the non-local constitutive relationship, the induced stress at a reference point can be considered to be a function of the strain field at every point in the material [38] in accordance with the phonon dispersion using both lattice dynamics obtained for the atomic model and experimental observations. Based on the stress-driven model [39], the non-local relationship is adopted for the bending interaction field as an input variable and the curvature field as an output for the integral convolution of the averaging kernel and interaction field of bending. Strain gradient theory of non-local elasticity proves that wave propagation should not be matched with the experimental results based on the strain gradient model and non-local elasticity model [37]. Indeed, some authors have studied in detail clamped-free cantilever and clamped cantilevers. They aimed to examine bridge-based behavior usingthe stress-driven model and investigate non-local behavior on asmall scale, especially for the clamped-end where the constitutive boundary conditions have considerable influence [39–40].

However, some studies have employed non-local elasticity models for nanomaterials to derive the non-local Euler beam model based on standard Euler beam theory in which the influence of shear stiffness is ignored [28]. In fact, the calculated strain for axial buckling obtained using molecular mechanics do not correspond to the non-local formdue to shear stiffness that takes a notable role in determining the non-local dynamic behavior of nanobeam structures. To investigate the change in the dynamic behavior caused by non-local behavior [41], researchers have applied non-local elasticity to different materials [42–45]. They have modeled non-local dynamic behavior [46, 47]. Xu et al. [48] and Arani et al. [49] found that the non-local behavior of nanobeams reproduced both the natural frequency and amplitude coefficient. Ke et al. [46, 47] confirmed that the non-local parameter has a strong effect on the vibrational behavior. Bourouina et al. [50] developed an analytical model to investigate the frequency shift caused by adsorption phenomenon in an adatom-nanobeam system and verified the size-dependent nanobeam dynamic behavior.

Nowadays, perforated structures are common constituents in nanotechnology, particularly for the design of mechanic microdevices and nanophotonics applications [51–54]. Nevertheless, frequency shift analysis of these nanostructures has not

been investigated as broadly as standard nanostructures in spite of their diverse potential in emerging nanotechnology applications. In fact, the influence of nanoholes on the frequency shift has only been modeled for simple practical cases and applications due to the complex modeling required. Fras et al.[56] evaluated the breaking of a microstrength armor plate under loading. They found that the holes are below the impact fail areas due to shear induced by the loading force. Using a different technique, Orunand Guler [57] studied the influence of perforation strengthening on the buckling evolution of a beam structure in the presence of various effects. They concluded that the proposed structure has a convergence of 0.08 within the loading effect when compared with the shear force within a reaching effect.

Recently, an investigation onthe influence of perforation was interested in the ultrasonic Talbot effect andthe effect of the filling fraction [58] and vibration shift. Luschi et al. [59] have derived effective expressions for the micromechanical properties of perforated microbeams and have proposed a local form forthe vibration frequency. Eltaher et al. [60] found that non-local behavior and perforation parameters have an important influence on the static and dynamic behavior of nanobeams. Bourouina et al.[61] derived a non-local shift model combining Eringen's material elasticity and dynamic nanobeam theory to study both the bending and shear forces governing the dynamic vibration of a perforated nanobeam. However, only the influence of the perforation parameters has been modeled, and not the adsorption phenomenon. Kerid et al. [62] modeled, the influence of thermal and magnetic loading on the vibration shift of perforated nanobeams on a small scale. They also found that the small-scale effects cannot be omitted for nanometric dimensions at higher mode numbers, while other studies have analyzed the local frequency shift depending on the relative density of the distributed mass and nanobeam dimensions. However, the influence of adsorption on the vibration shift in conjunction with perforation has never been addressed.

On the other hand, an investigation on the shear stiffness effect on the nanobeam vibration in the presence of distributed adatoms has been studied for full structures only. According to the previously reported studies[59,60], the bending stiffness is related to the perforation parameters and thus, the frequency shift can be affected due to the influence of the square hole network. Indeed, the equivalent bending stiffness varies as a function of both the number and size of holes. Moreover, the shear stiffness and perforation parameters are related to the change inthe equivalent geometry of the nanobeam structure and thus, the dynamic behavior can be affected by the square hole network [59,61]. However, the effect of the distributed adatoms on the non-local frequency shift in conjunction with thesquare hole network has never been studied.

In this work, standard beam vibration and Eringen's material elasticity theories were applied in conjunction with the interaction potential. The present work introduces both bending and shear stiffness to investigate the dynamic behavior of the nanobeam structure with distributed adatoms where both the shear and Euler beam models were developed considering the vdW interaction energy effect using Lennard-Jones (6-12) potential. The small scale effect was also modeled in the present study to determine the non-local frequency shift at nanometric dimensions. In addition, both the vdW interaction energy between the adsorbed atoms and vdW interaction energy between the adsorbed atoms and the nanobeam structures atoms were considered in order to calculate the total induced energy. The purpose of this study was to model the influence of perforation and adsorption on the induced non-local frequency shift for an adatom-perforated nanobeam system based on a structure containing aperiodic square hole network. Consequently, this paper initially deals with calculating the adsorption-induced energy. Subsequently, explicit dynamic equations were developed using thenon-local material elasticity including the adsorption phenomenon effect. Finally, both perforation and adsorption on the non-local shift were investigated by performing calculations and detailed discussions presented.

2. Problem formulation

In order to develop the vibration equations with the adsorbate, anon-local approach to theelasticity wasused in which the bending and shear forces can be expressed using anon-local version [50]. The vibration dynamics of the perforated nanostructure will be modeled using non-local elasticity and shear beam theory containing the effective characteristic parameters for shear and bending forcesto derive the adsorption induced non-local shift.

2.1. System dynamic behavior

In this context, we consider a nanostructure of length L, width b and thickness $2h$, perforated with a network of periodic square holes of spatial period (s_P) and size (d_h), as presented in Fig.1a. We define N as the number of holes along the section, and $\beta=(d_h/s_P)$ as the hole size ratio ranging from 0 (full structure) to 1, as shown in Fig.1b.

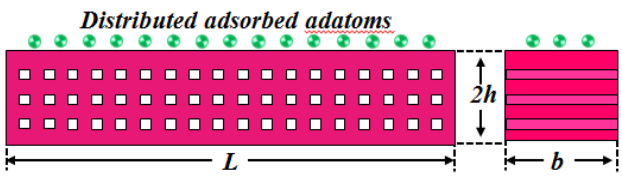

(a)

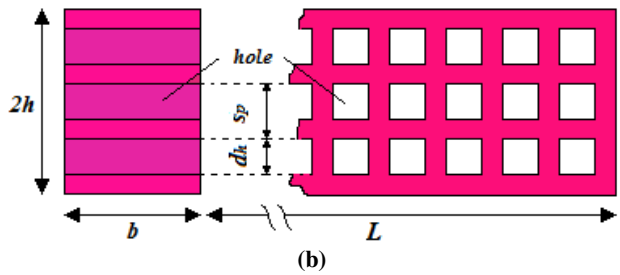

Fig.1. The model of the adatom-nanobeam system: **(a)** The perforated nanobeam structure containing adatoms distributed on its upper surface and **(b)** the geometry of the perforated nanobeam structure containing aperiodic square hole network.

Luschi and Pieri [62] calculated the theoretical expression for the equivalent value of the mass per unit of length (ρA_{eq}) and the equivalent value of the rotation inertia per unit of length (ρI_{eq}) with respect to the mass per unit of length (ρA_f) and the rotation inertia per unit of length (ρI_f) for the full structureas follows:

$$\rho A_{eq} = \rho A_f \, \chi_m(\alpha, N) \tag{1a}$$

$$\rho I_{eq} = \rho I_f \, \chi_r(\alpha, N) \tag{1b}$$

Where $\chi_m(\alpha,N)$ and $\chi_r(\alpha,N)$ can be calculated as a function of the number of holes (N) and the filling ratio [$\alpha=(1-\beta)$] using the following equations:

$$\chi_m(\alpha, N) = \frac{(1 - N(\alpha - 2))\alpha}{(N + \alpha)} \tag{2a}$$

$$\chi_r(\alpha, N) = \frac{\alpha((2-\alpha)N^3 + 3N^2 - 2(\alpha-3)(\alpha^2 - \alpha + 1)N + \alpha^2 + 1)}{(N+\alpha)^3} \tag{2b}$$

To develop the vibration equations with the adsorbates, anon-local approach to the elasticity was used where the bending and shear forces can be expressed using alocal version. Considering the interaction energy in the Lagrangian function of the system using Hamilton's principle [50], the governing equations for the vibration of the adatom-nanobeam system are given by combining the equations in the terms of the deformation (w) and rotation (ψ) as follows [50]:

$$\frac{\partial V}{\partial x} - \left(\rho A_{eq} + \eta b m_a\right)\frac{\partial^2 w}{\partial t^2} - \eta b \phi \frac{\partial^4 w}{\partial x^4} = -H\gamma \tag{3a}$$

$$\frac{\partial M}{\partial x} + V = \rho I_{eq} \frac{\partial^2 \psi}{\partial t^2} \tag{3b}$$

where V is the shear force at deformation, M is the bending moment for the structure, m_a is the adatom mass and η is the adsorption density. According to the Laplace-Young equation [53], the load (Hk) is due to the residual surface stress (τ_0) in the deformed nanobeam with $H=2\tau_0 b$ and $\gamma=(\partial^2 w/\partial x^2)$ for rectangular cross-sections [50]. The parameter, $\phi = \left[\partial^2 p^{vdW}/\partial\gamma^2\right]_{\gamma=0}$, in Eq.3a was determined when the curvature of the perforated structure equals zero ($\gamma=0$) and the quantity $p^{vdW} = (p^{vdW}_{MM'} + 2p^{vdW}_{M1(M3)})$ is the total vdW energy, where p^{vdW}_{MM} is the vdW energy between adsorbed atoms and M,M' and $p^{vdW}_{M1(M'3)}$ are the vdW energy between an adsorbed atom M (or M'atom) and structure atom 1 (or atom 3), respectively (Fig.2). The vdW energy (p^{vdW}_{MM}) between adatoms M and M' is given by:

$$p^{vdW}_{MM'} = -A_2\{d\,[1 + (h + a)k]\}^6 + B_2\{d\,[1 + (h + a)k]\}^{12} \tag{4}$$

The vdW energy between an adsorbed atom M and structure atom 1 (or between M' and 3) can be expressed as follows [50]:

$$p_{M1(M'3)}^{vdW} = -A_1\left\{a^2 + \left[(1/4)c^2(1+hk)^2\right]\right\}^{-3} + B_1\left\{a^2 + \left[(1/4)c^2(1+hk)^2\right]\right\}^{-6} \tag{5}$$

For a small value, P^{vdW} can be approximated by the Taylor serial expansion for the initial structure state:

$$P^{vdW} = p^{vdW}\Big|_{\gamma=0} + \frac{\partial p^{vdW}}{\partial \gamma}\Big|_{\gamma=0}\gamma + \frac{1}{2}\frac{\partial^2 p^{vdW}}{\partial \gamma^2}\Big|_{\gamma=0}\gamma^2 \tag{6}$$

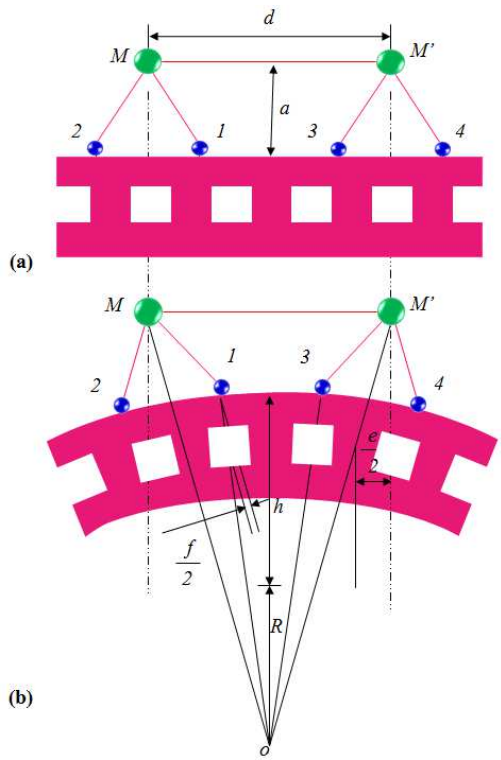

Fig. 2. The adatom-nanobeam system during the adsorption phenomena of distributed adatoms: **(a)** The system at equilibrium and **(b)** the system under deformation.

The expressions for both the bending moment (M) and shear force (V) on a small-scale should be given by the non-local expressions including the corrective parameter proposed by Eringen [50]. Thisisdue to the total behavior of the nanobeam structure at nanometric dimensions. Thus, the non-local version of the expressions for M and V are defined by Eq.7a and Eq.7b, respectively:

$$M = (e_0 a)^2 \frac{\partial^2 M}{\partial x^2} + EI_{eq}\frac{\partial \psi}{\partial x} + 2Sbh^2\frac{\partial \psi}{\partial x} \tag{7a}$$

$$V = (e_0 a)^2 \frac{\partial^2 V}{\partial x^2} + \gamma GA_{eq}\frac{\partial w}{\partial x} - \gamma GA_{eq}\psi \tag{7b}$$

where $(e_0a)^2$ is the non-local parameter revealing the small scale effect, $\gamma$is the shear factor equal to 5/6 [64], and S is the surface elastic constant. The material parameters EI_{eq} and GA_{eq} are the equivalent bending and shear stiffnesses, defined with respect to the bending (EI_f) and shear (GA_f) stiffnesses of the full structure using Eq.8a and Eq.8b, respectively:

$$EI = EI_f\,\chi_b(\alpha, N) \tag{8a}$$

$$GA = GA_f\,\chi_s(\alpha, N) \tag{8b}$$

With $\chi_b(\alpha,N)$ and $\chi_s(\alpha,N)$, which are the functions related to the influence of the filling ratio (α) and the number of holes (N),they can be calculated as follows:

$$\chi_b(\alpha,N)=\frac{(N+1)\alpha(N^2+2N+\alpha^2)}{(1-\alpha^2+\alpha^3)N^3+3\alpha N^2+(3+2\alpha-3\alpha^2+\alpha^3)\alpha^2 N+\alpha^3} \tag{9a}$$

$$\chi_s(\alpha,N)=\frac{(N+1)}{N}\alpha^2 \tag{9b}$$

For many practical cases, it can be shown that the rotation effect term (ρI_{eq}) is 3–6 times smaller than the shear deformation term $(EI_{eq}.\rho A_{eq}/kAG_{eq})$ [61]. Hence the term $\rho I_{eq}.\ \partial^2\psi/\partial t^2$ can be neglected from the second Timoshenko beam equation. Thus, the complete solution is not required and only the bending and shear effects are considered. Therefore, Eq.3 is modified to the shear beam equation and reduced to the following equation:

$$\frac{\partial V}{\partial x}-\left(\rho A_{eq}+\eta b m_a\right)\frac{\partial^2 w}{\partial t^2}-\eta b\phi\frac{\partial^4 w}{\partial x^4}=-H\gamma \tag{10a}$$

$$\frac{\partial M}{\partial x}+V=0 \tag{10b}$$

Now, substituting Eq.7a and Eq.7b into Eq.10a and Eq.10b gives the non-local version of the expression for M and V as follows:

$$M=\left(EI_f\chi_b+Sbh^2\right)\frac{\partial\psi}{\partial x}+\left(e_0a\right)^2\left[\left(\rho A_f\chi_m+\eta b m_a\right)\frac{\partial^2 w}{\partial t^2}+2\tau_0 b\frac{\partial^2 w}{\partial x^2}-\eta b\phi\frac{\partial^4 w}{\partial x^4}\right] \tag{11a}$$

$$V=\gamma GA_f\chi_s\left(\frac{\partial w}{\partial x}-\psi\right)+\left(e_0a\right)^2\left[\left(\rho A_f\chi_m+\eta b m_a\right)\frac{\partial^3 w}{\partial x\partial t^2}-2\tau_0 b\frac{\partial^3 w}{\partial x^3}+\eta b\phi\frac{\partial^5 w}{\partial x^5}\right] \tag{11b}$$

Eq.11a corresponds to the explicit non-local expression forthe bending moment for an adatoms-nanobeam system based on a perforated structure with a square hole network and Eq.11b corresponds to the explicit non-local expression forthe shear force during the deformation of the system. For a negligible adatom density $(\eta\rightarrow 0)$, these expressions are reduce to the explicit expressions of M and V for standard nanobeams:

$$M=(EI_f\chi_b+Sbh^2)\frac{\partial\psi}{\partial x}+\left(e_0a\right)^2\left[\rho A_f\chi_m\frac{\partial^2 w}{\partial t^2}+2\tau_0 b\frac{\partial^2 w}{\partial x^2}\right] \tag{12a}$$

$$V=\gamma GA_f\chi_s\left(\frac{\partial w}{\partial x}-\psi\right)+\left(e_0a\right)^2\left[\rho A_f\chi_m\frac{\partial^3 w}{\partial x\partial t^2}-2\tau_0 b\frac{\partial^3 w}{\partial x^3}\right] \tag{12b}$$

2.2. Non-local frequency shift

In this subsection, the non-local shift caused by adsorption has been developed. Two models were considered: The Shear beam model (SBM) and Euler beam model (EBM). For a small deformation of the nanobeam vibrations, simply-supported nanobeams are typical nanostructures encountered in design problems [65]. An analytical approach was developed for the frequency shift of a perforated nanobeam using Timoshenko nanobeam theory with Eringen'snon-local theory. Since the adatom-nanobeam system is considered as a simply-supported system, both the deformation and rotation have to satisfy Navier's solution [66, 67]. Substituting Eq.12a and Eq.12b into Eq.10a and Eq.10b, the explicit non-local expression of the system coupled equations for the Timoshenko nanobeam with adsorbed adatoms and small scale effects is:

$$\gamma GA_f\chi_s\frac{\partial}{\partial x}\left[\frac{\partial w}{\partial x}-\psi\right]+2\tau_0 b\frac{\partial^2}{\partial x^2}\left[w-\left(e_0a\right)^2\frac{\partial^2 w}{\partial x^2}\right]=(\rho A_f\chi_m$$
$$+\eta b m_a)\frac{\partial^2}{\partial t^2}\left[w-\left(e_0a\right)^2\frac{\partial^2 w}{\partial x^2}\right]+\eta b\phi\frac{\partial^4}{\partial x^4}\left[w-\left(e_0a\right)^2\frac{\partial^2 w}{\partial x^2}\right] \tag{13.a}$$

$$(EI_f\chi_b+Sbh^2)\frac{\partial^2\psi}{\partial x^2}+\gamma GA_f\chi_s\left(\frac{\partial w}{\partial x}-\psi\right)=0 \tag{13.b}$$

Differentiating Eq.13a with respect to position x and substituting $\partial\psi/\partial x$ from Eq.13b yields the non-local differential equation using shear beam theory as follows:

$$\left\{\frac{\left[(EI_f\chi_b+Sbh^2+2\tau_0 b(e_0a)^2+\eta b\phi)(\gamma GA_f\chi_s)\right]+\left[2\tau_0 b(EI_f\chi_b+Sbh^2+\eta b\phi)\right]}{(\rho A_f\chi_m+\eta bm_a)}\right\}\frac{\partial^4 w}{\partial x^4}$$
$$-\left\{\frac{2\tau_0 b}{(\rho A_f\chi_m+\eta bm_a)}\right\}\frac{\partial^2 w}{\partial x^2}+\left\{\frac{\left(EI_f\chi_b+Sbh^2+\eta b\phi\right)-\left[((e_0a)^2\gamma GA_f\chi_s)\right]}{(\gamma GA_f\chi_s)}\right\}\frac{\partial^4 w}{\partial x^2\partial t^2}+$$
$$-\left\{\frac{2\tau_0 b(e_0a)^2\left(EI_f\chi_b+Sbh^2+\eta b\phi\right)}{(\rho A_f\chi_m+\eta bm_a)\gamma GA_f\chi_s}\right\}\frac{\partial^6 w}{\partial x^6}+\left\{\frac{\left(EI_f\chi_b+Sbh^2+\eta b\phi\right)}{\gamma GA_f\chi_s}\right\}\frac{\partial^6 w}{\partial x^4\partial t^2}+\frac{\partial^2 w}{\partial t^2}=0 \quad (14)$$

For small deformations, simply-supported nanobeams are the typical structures encountered in theoretical problems [65]. Since the adatom-nanobeam system is considered a simply-supported system, the deformation has to satisfy Navier's solution [66, 67]. When considering a deformation solution for the harmonic form ofthe vibration of a perforated system, the deflection (w) of the adatoms-nanobeam system can be given as follows [15,50,61,68]:

$$w_n(x,t)=w_{\max}\sin(\kappa_n x)\cos(\omega_n t) \quad (15)$$

where w_{max} denotes the deflection amplitude, $\kappa_n=n\pi/L$ is the wavenumber and ω_n is the n-*th* pulsation. Consequently, substituting Eq.15 into Eq.14 gives the non-local pulsation equation for the n-*th* vibration mode of the adatom-microbeam system including the effects of the periodic square hole network. Therefore, the non-local vibration frequency obtained using the SBM can beexpressed as follows:

$$(\omega_n^2)_s^a=\frac{\xi_4^a\kappa_n^6-\xi_1^a\kappa_n^4+\xi_2^a\kappa_n^2}{1-\xi_5^a\kappa_n^4+\xi_3^a\kappa_n^2} \quad (16)$$

where the coefficients $\xi_1^a$to ξ_5^a are given by:

$$\xi_1^a=\frac{(EI_f\chi_b+Sbh^2+2\tau_0 b(e_0a)^2+\eta b\phi)\gamma GA_f\chi_s+2\tau_0 b(EI_f\chi_b+Sbh^2+\eta b\phi)}{\rho A_f\chi_m+\eta bm_a} \quad (16a)$$

$$\xi_2^a=-\frac{2\tau_0 b}{\rho A_f\chi_m+\eta bm_a} \quad (16b)$$

$$\xi_3^a=-\frac{(e_0a)^2\gamma GA_f\chi_s-EI_f\chi_b-Sbh^2-\eta b\phi}{\gamma GA_f\chi_s} \quad (16c)$$

$$\xi_4^a=-\frac{2\tau_0 b(e_0a)^2(EI_f\chi_b+Sbh^2+\eta b\phi)}{(\rho A_f\chi_m+\eta bm_a)\gamma GA_f\chi_s} \quad (16d)$$

$$\xi_5^a=\frac{EI_f\chi_b+Sbh^2+\eta b\phi}{\gamma GA_f\chi_s} \quad (16e)$$

Therefore, the non-local frequency shift expression for the SBM model can be calculated as follows:

$$(\Delta\omega_n)_s^a=(\omega_n)_s^a-(\omega_n)_s^o \quad (17)$$

where $(\omega_n)_s^o$ is the non-local resonance frequencies obtained using the SBM for a standard nanobeam *($\eta\rightarrow 0$)* calculated as follows:

$$(\omega_n^2)_s^o=\frac{\xi_4^o\kappa_n^6-\xi_1^o\kappa_n^4+\xi_2^o\kappa_n^2}{1-\xi_5^o\kappa_n^4+\xi_3^o\kappa_n^2} \quad (18)$$

where the coefficients ξ_i^o for i=1to 5 are related to the coefficients ξ_i^a using:

$$\xi_i^o = \xi_i^a \Big)_{\eta=0} \quad (19)$$

To determine the dynamic equation, the shear parameter [62] should be much less than unity, $EI_{eq}/(GA_{eq}L^2) << 1$. When the contribution from the shear effect is neglected, the equation should be replaced by theequation used for the EBM with non-local behavior as follows:

$$\frac{2\tau_0 b(EI_f\chi_b + Sbh^2 + \eta b\phi)}{\rho A_f\chi_m + \eta b m_a}\frac{\partial^4 w}{\partial x^4} - \frac{2\tau_0 b}{(\rho A_f\chi_m + \eta b m_a)}\frac{\partial^2 w}{\partial x^2} - (e_0 a)^2\frac{\partial^4 w}{\partial x^2 \partial t^2} + \frac{\partial^2 w}{\partial t^2} = 0 \quad (20)$$

Considering a deformation solution with aharmonic form for the vibration system, like theSBM model, and assuming the effect of shear distortion was negligible, the condition of solution w_{max} of Eq.15 gives the vibration frequency as follows:

$$(\omega_n^2)_e^a = \frac{\zeta_1^a \kappa_n^4 - \zeta_2^a \kappa_n^2}{1 + \zeta_3^a \kappa_n^2} \quad (21a)$$

$$\zeta_1^a = \frac{2\tau_0 b(EI_f\chi_b + Sbh^2 + \eta b\phi)}{\rho A_f\chi_m + \eta b m_a} \quad (21b)$$

$$\zeta_2^a = -\frac{2\tau_0 b}{(\rho A_f\chi_m + \eta b m_a)} \quad (21c)$$

$$\zeta_3^a = (e_0 a)^2 \quad (21d)$$

Therefore, the non-local frequency shift expression for the EBM can be calculated as follows:

$$(\Delta\omega_n)_e^a = (\omega_n)_e^a - (\omega_n)_e^o \quad (22)$$

where $(\omega_n)_s^o$ is the non-local resonance frequencies obtained using the SBM for a standard nanobeam $(\eta \to 0)$ calculated as follows:

$$(\omega_n^2)_e^a = \frac{\zeta_1^o \kappa_n^4 - \zeta_2^o \kappa_n^2}{1 + \zeta_3^o \kappa_n^2} \quad (23)$$

The coefficients ζ_i^o for $i=1$ to 5 are related tothe coefficients ζ_i^a as follows:

$$\zeta_i^o = \zeta_i^a \Big)_{\eta=0} \quad (24)$$

3. Results and discussion

We computed and examined the non-local vibration frequency shift by changing the filling ratio, $\alpha = (1-\beta)$, the number of square holes, density of distributed adatoms and nanobeam thickness for a rectangular perforated nanostructure constructed from *Au* (100) with the geometrical parameters $(L,b,h)=(100\ nm,\ 10\ nm,\ 10\ nm)$. In addition, the material parameters were E = 78600 MPa, ρ = 19300 kg/m^3, S = 32.9 eV/nm^2, τ_0 = 140 N/cm and $\mu = e_o a/L$ = 0.2 [50,62]. These values allow calculation of the mechanical parameters EI_{eq}, GA_{eq}, and ρA_{eq} versus the number N and α. Computation was carried out with MATLAB code for a perforated microbeam of one square hole (N=1) per section and β value from 0 to 0.9. Other analyses were completed in the N range from 1 to 10 to examine its effect on the calculated shift. The interatomic interaction parameters of the H adatoms are gathered in Table1.

Table 1. The physical parameters used in the calculation for the adsorption of H adatoms [50].

Parameters	H/Au (100)	Unit
m_a	1.660×10^{-27}	kg
c	0324×10^{-12}	m
a	0251×10^{-12}	m
A_1	04945×10^{-82}	Jm^6
B_1	2123×10^{-139}	Jm^{12}
A_2	3536×10^{-82}	Jm^6
B_2	1022×10^{-139}	Jm^{12}

The adsorption effect influences the vibration frequency of the perforated system is better illustrated by defining the shift ratio as follows:

$$\beta_{s,e}^{a} = \frac{(\Delta\omega_n)_{s,e}^{a}}{(\omega_n)_{s,e}^{o}} = \frac{(\omega_n)_{s,e}^{a} - (\omega_n)_{s,e}^{o}}{(\omega_n)_{s,e}^{o}} \tag{13}$$

3.1. Influence of perforation parameters

The evolution of the vibration frequency shift obtained usingthe SBM and EBM is shown in Fig.3. This is versus the β value for two values of number N and density Θ. The vibration shift for the perforated system ($\beta \neq 0$) stands out clearly when compared to the shiftin the full system ($\beta = 0$) over the β range studied in both the SBM and EBM. These results confirm those reportedin the literature [62] concerning the influence of the perforation parameter β on the mechanic behavior of perforated nanostructures. In addition, a decrease in the shift was observed including the density Θ and number N when compared to those without the effect of these parameters as already noted in Ref.[50]. For both the SBM and EBM, an increase in the mode number from the fundamental mode (Fig.3a and c) to the second mode (Fig.3b and d) increases the shift over the β range studied. This behavior comes from the influence of the total adsorbed mass of the distributed adatoms plus the total adsorption.

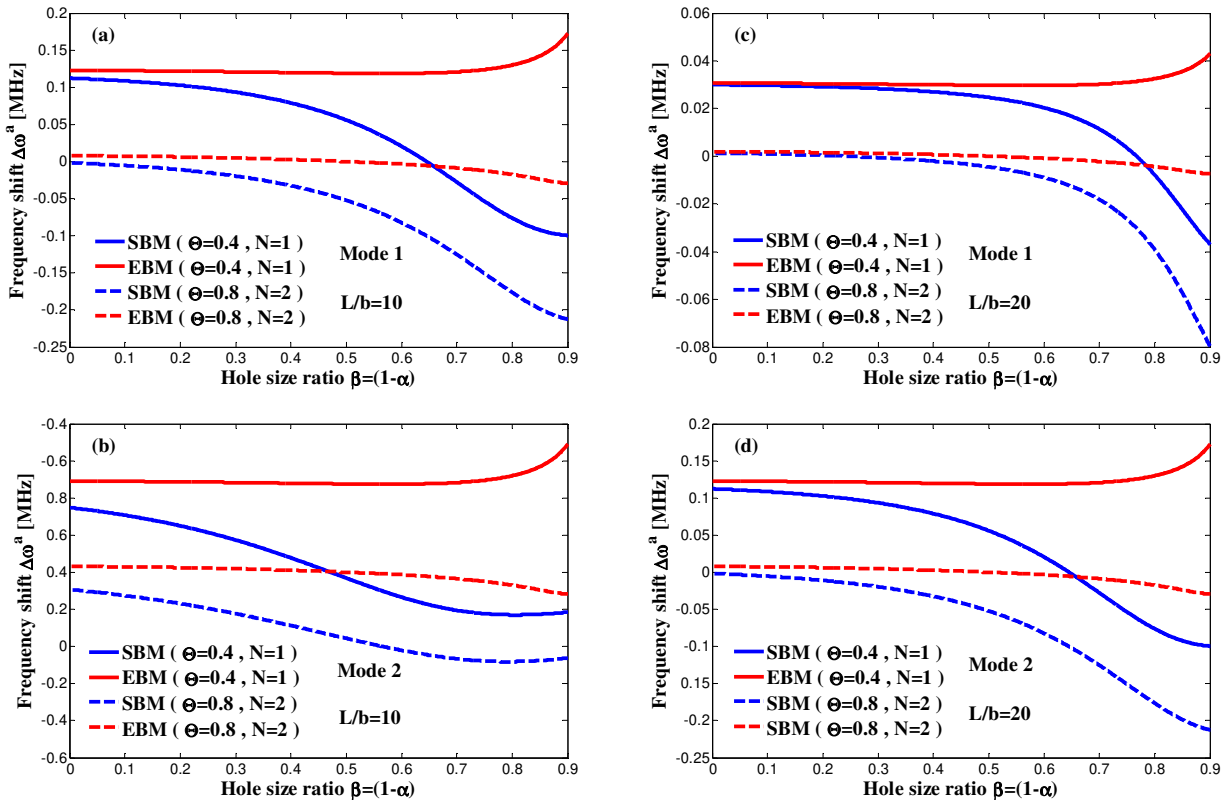

Fig.3. Frequency shift versus β for two values of N and Θ

with $h=10nm$: $L/b=10$ for **(a)** mode 1 and **(b)** mode 2; $L/b=20$ for **(c)** mode 1 and **(d)** mode 2.

Table 2 presents the calculated fundamental frequency for the adatoms-nanobeam system based on the shear and Euler beam models for $N=1$, $\Theta=0.5$ and different hole size ratios (β). A decrease in the vibration frequency can be obtained when the non-local parameter is considered for both the SBM and EBM, which translate the non-local behavior of the adatoms-nanobeam system. In addition, the calculated value for the frequency shift using the SBM is lower than the calculated value obtained using the EBM over the β range studied. It is also lower when the ratio (L/b) increases from 10 (Fig.3a and b)) to 20 (Fig.3c and d) as a translation for the reduction in the total mass influence with respect to an increase in the system dimensions. In addition, as shown in Fig.3, the calculated shift obtained using the EBM increases when the β value increases whether it includes or excludes density and number effects. This is a result of the influence of effective bending [50], which varies in a proportional relationship with $\chi_s(\alpha,N)/\chi_m(\alpha,N)$ value. Similarly, the calculated shift within the SB model depends on the shear effect [50], which varies proportionally with the $\chi_s(\alpha,N).\chi_m(\alpha,N)/\chi_s(\alpha,N)$ value. Therefore, since this last term increases with the β value, the difference in the calculated frequency obtained using the SBM and EBM increases with the β value. Moreover, since the term is not equal to zero ($\chi_s(\alpha,N).\chi_m(\alpha,N)/\chi_s(\alpha,N) \neq 0$), the calculated shift curves versus β obtained using the SBM and EBM can never converge for the perforated nanobeam ($\beta\neq0$)or full nanobeam ($\beta=0$).

Table 2. The fundamental frequencies *[GHz]* obtained for the adatoms-nanobeam system based on the shear beam and Euler beam models for $N=1$ and $\Theta=0.5$.

Hole size ratio	*System model*	*L/b =10*		*L/b =20*	
		Large-scale $\mu=0$	Small-scale $\mu=0.2$	Large-scale $\mu=0$	Small-scale $\mu=0.2$
$\beta = 0.1$	SBM	11.110807	11.109249	2.831674	2.830548
	EBM	11.401505	11.400971	2.850376	2.849213
$\beta = 0.2$	SBM	11.086614	11.085293	2.847575	2.846439
	EBM	11.497216	11.498047	2.874304	2.873227
$\beta = 0.3$	SBM	11.063423	11.062550	2.876968	2.875807
	EBM	11.668366	11.667147	2.917091	2.915946
$\beta = 0.4$	SBM	10.991504	10.989178	2.917387	2.915132
	EBM	11.925063	11.923420	2.981265	2.979091
$\beta = 0.5$	SBM	10.766695	10.764731	2.960246	2.958101
	EBM	12.277461	12.275289	3.069365	3.067138

Fig.4 presents the calculated shift obtained using the SBM and EBM versus N for two values of β and Θ. A decrease in the vibration shift was obtained when N increases for both the SBM and EBM. This is a result of the decrease in $\chi_s(\alpha,N)/\chi_m(\alpha,N)$ and $\chi_s(\alpha,N).\chi_m(\alpha,N)/\chi_s(\alpha,N)$ for both mode 1 (Fig.4a and c) and mode 2 (Fig.4b and d), respectively. In addition, for the EBM, the frequency shift becomes lower than frequency shift corresponding to the case of full system ($\beta=0$), particular,when $N > 2$ [62]. This indicates that for larger numbers, the influence of effective bending on perforated systems with a network of periodic square holes becomes lower than the influence of effective bending effect on their corresponding full systems.

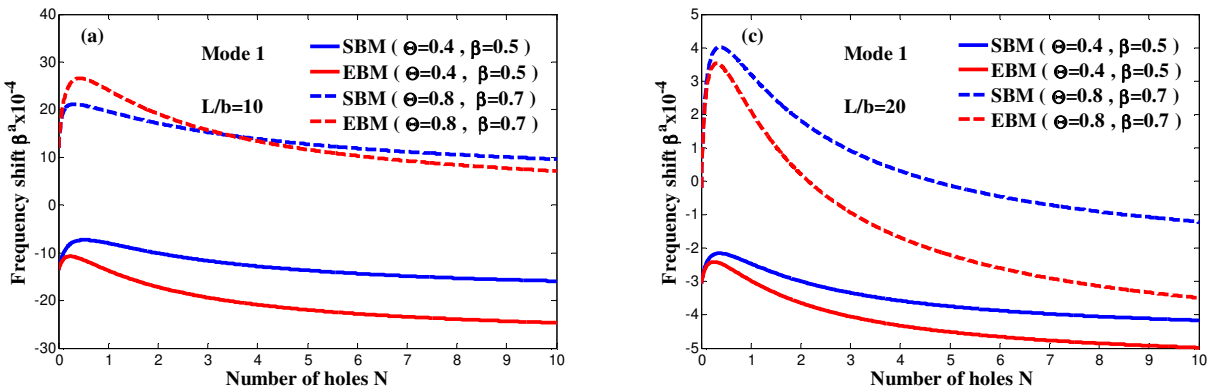

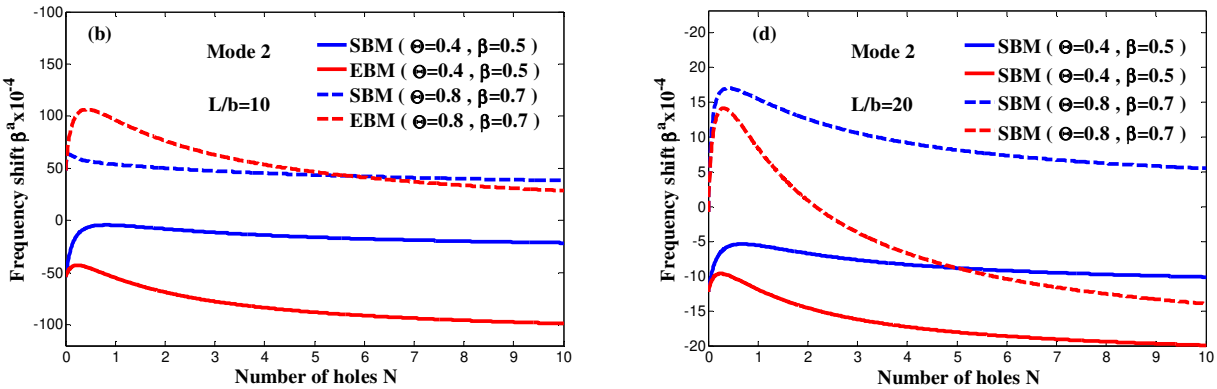

Fig.4. Frequency shift versus *N* for two values of *β* and *Θ* with: *h=10nm,L/b=10* for**(a)** mode 1 and **(b)** mode 2; *L/b=20* for**(c)** mode 1 and**(d)** mode 2.

Table 3 shows the calculated frequency for the fundamental mode of vibration for the adatoms-nanobeam system based on the shear beam and Euler beam models for *β =0.5*, *Θ=0.5* and different numbers of holes *N*. The presented results demonstrate a reduction in the fundamental frequency for non-local bending and non-local shear with respect to the local models. This shows the small scale effect on the dynamic behavior of the adatoms-nanobeam system. In addition, the estimated value of the frequency shift through the SBM is less than that estimated using the EBM when the length-to-width ratio *L/b* increases due to the influence of the total adsorbed adatoms with respect to anincrease in the system dimensions.

Table 3. Fundamental frequencies *[GHz]* for the adatoms-nanobeam system based on the shear beam and Euler beam models for *β=1* and *Θ=0.5*.

Number of holes	*System model*	*L/b =10*		*L/b =20*	
		Large-scale *μ=0*	Small-scale *μ=0.2*	Large-scale *μ=0*	Small-scale *μ=0.2*
N = 1	SBM	10.766695	10.764731	2.960246	2.958101
	EBM	12.277461	12.275289	3.069365	3.067138
N = 2	SBM	10.007266	10.006471	2.782448	2.781271
	EBM	11.597154	11.596207	2.899288	2.898942
N = 3	SBM	9.625747	9.624519	2.683458	2.682117
	EBM	11.197868	11.196370	2.799467	2.798732
N = 4	SBM	9.397154	10.989178	2.621754	2.619179
	EBM	10.944200	10.942736	2.736050	2.734517
N = 5	SBM	9.244899	9.242517	2.579795	2.577230
	EBM	10.770025	10.768369	2.692506	2.690752

For the SBM, the calculated shift also becomes lower than that corresponding to thefull system dueto the influence of shear when *N* increases from 0 to 10 whether it includes or excludes adsorbed adatoms. However, increasing the number of modes (*n*) increases the vibration shift. This is due to the increase in the frequency with *n* as noted in Ref.[62]. Moreover, since the influence of shear increases with *N,* the difference between the calculated frequencies versus the SBM and EBM increases with *N.*

3.2. Influence of geometrical parameters

The non-local parameter determines the small-scale effect onthe dynamic behavior [6, 28]. According to Eringen's elasticity theory, this parameter is an appropriate constant for nanobeam materials calculated by comparing the lattice dynamic results with those of the non-local theory. Fig.5 represents the relative shifts obtained using SBM and EBM versus the system thickness (*2h*) for the full *(β, N)= (0,0)* and perforated *(β, N)=(0.718,1)* systems, respectively. The relative shift in frequency obtained using the SBM was *20* (Fig.5c and d) due to the reduction in the total mass of H adatoms with respect to an increase in the system's dimensions. On the other hand, the variation in the vibration frequency can be justified by the following explanation: The non-local behavior observed at nanometric dimensions makes the adatoms-nanobeam system more flexible and thus, the non-local elasticity model should be applied for more predictions of high values of vibration frequencies on asmall-scale [3, 38].

As can be seen, for both mode 1 and mode 2, the shift obtained using the SBM is less than thatfound using the EBM over the whole thickness (*2h*) for both the standard and perforated system and for both mode 1 (Fig.5a and c) and mode 2 (Fig.5b and d). This latter reduction corresponds to the influence of shear on the mechanic behavior of the perforated system

[61]. Also, the induced frequency shift can be considered as an indicator to estimate the non-local behavior ofthe adatoms-nanobeam system. Figure 1 and 2 showthe frequency shift is less than unity for both the first and second modes of vibration. This means that the SBM of the perforated nanobeam leads to an over augury of the vibration when the small-scale effect is ignored in the structure of the adatoms-nanobeam system.

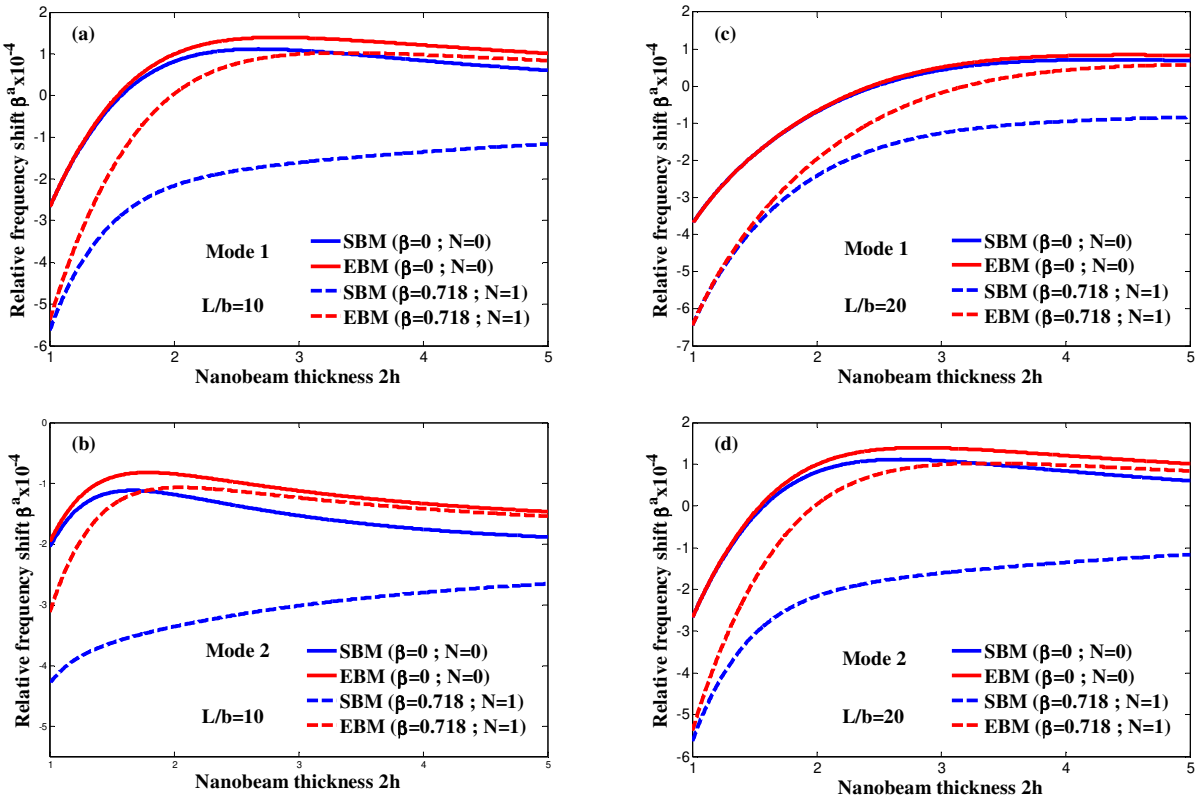

Fig.5. The frequency shift versus thickness *(2h)* for the full *(β,N)=(0,0)* and perforated *(β,N)=(0.718,1)* systems with *Θ=1*: *L/b=10* for **(a)** mode 1 and **(b)** mode 2; *L/b=20* for **(c)** mode 1 and **(d)** mode 2.

The value of the frequency shift is also strongly affected by H adatoms. If we neglect the additional effect of H adatoms, the frequency expression developed using the EBM will be limited to estimating the influence of adsorption phenomena. Furthermore, for both the SBM and EBM, the perforation structure increases the shift when compared to that found without perforation, particularly for mode 2 at a low system thickness. This can be attributed to anincrease in the frequency with mode *n* as cited in Ref.[61,62]. Moreover, the periodic square holes network makes the perforated system softer when the thickness increases when compared to that of the standard system with the same dimensions. In addition, the variation in the calculated value of the frequency shift was amplified for mode 2 with respect to mode 1. A similar conclusion can be drawn when the length-to-thickness ratio was increased. In fact, the effect of the shear stiffness leads to a variation in the calculated value of the fundamental frequency [3, 37]. Thus, when the length-to-thickness ratio is small, the non-local shear beam model should be used for a suitable prediction of the dynamic vibration instead of the non-local EBM, which ignores the shear stiffness effects.

3.3. Influence of relative density

Fig.6 shows the plot of the relative shift obtained using the SBM and EBM versus density *Θ* for the full *(β,N)=(0,0)* and perforated *(β,N)=(0.718,1)* systems. For both mode 1 (Fig.6a and c) and mode 2 (Fig.6b and d), the use of perforation reducesthe relative shift whenthe density *(Θ)* increases due to the variation inequivalent bending with respect to the perforated system. In addition, the computed value obtained using the SBM was reduced more with respect of that obtained using the EBM regardless of the *Θ* value. These results confirm those presented in Ref. [69] which noteda similar interpretation, given the effect of the effective shear $[\chi_b(\alpha,N).\chi_m(\alpha,N)/\chi_s(\alpha,N)]$ on the system dynamics. Upon increasing *Θ*, the form of the traced curves including the effect of perforation was similar of that of the full system containing H/Au(100). So, varying *Θ* produces a curve in same way as represented in Ref.[50].

In fact, the relative shift was attributed to the following mechanisms: The variations in the total mass per unit of length and total bending stiffness, in which an agreement between these mechanisms gives the relative shift variation versus the relative density *Θ* [50]. Indeed, the total mass increases from $\rho A\chi_m$ to $\rho A\chi_m+\eta bm_a$ due to the adsorption phenomenon. Therefore, the

mass influence lowers the vibration frequency. In addition, the total bending changes from $EI\chi_b+Sbh^2$ to $EI\chi_b+Sbh^2+\eta b\phi+2\sigma_0 b(e_0a)^2$ and as an alternative, the bending influence increases the vibration frequency. Thus, the variation in mass and bending can explain the shift in the frequency versus the Θ value. The occurrence of these mechanisms leads to the variation in which the two maximum relative shifts obtained using the SBM and EBM can be represented in Fig.6a and b. Moreover, a critical density can be computed when no shift $\beta_a=0$ was observed. In this situation, the total mass annuls the total bending.

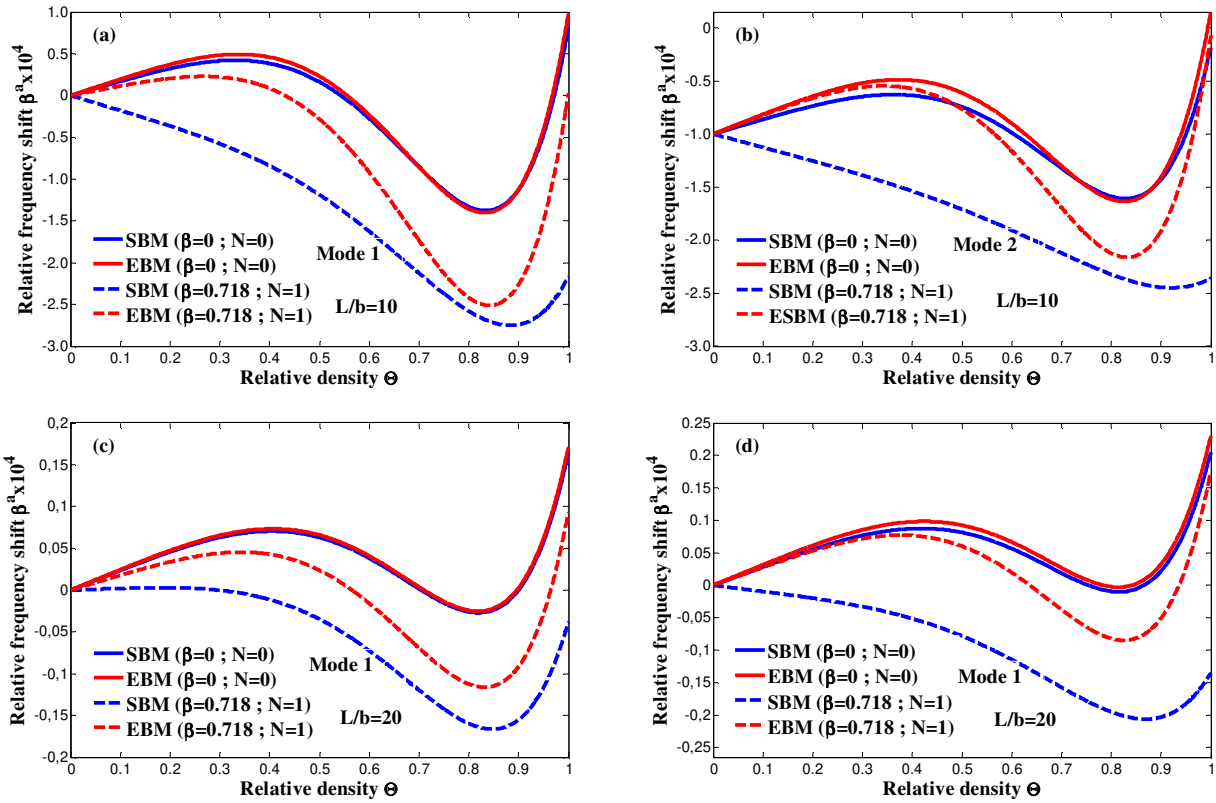

Fig.6. The frequency shift versus Θ obtained for the full $(\beta,N)=(0,0)$ and perforated $(\beta,N)=(0.718,1)$ systems with $h=10nm$: $L/b=10$ for **(a)** mode 1 and **(b)** mode 2; $L/b=20$ for **(c)** mode 1 and **(d)** mode 2.

4. Conclusions

In this paper, new adatom-nanobeam system perforated with a network of periodic square holes was analyzed and investigated on the basis of dynamic vibration theory and non-local material elasticity. The analytical expression for thevibration frequency obtained from the SBM and EBM were derived using a modification of the Timoshenko nanobeam theory. This has been applied to model the effect of perforation on the non-local shift induced by adsorbed adatoms. Both the SBM and EBM have been developed considering the vdW interaction energy using Lennard-Jones (6-12) potential. It has been shown that for a β sub-range of onehole $(N=1)$ and twoholes $(N=2)$, the observed shift is larger than that accounting for a full adatom-nanobeam system. This is attributed to the variation in the $\chi_s(\alpha,N)/\chi_m(\alpha,N)$ value, whereas the shift is smaller when compared to that calculated for the full system. In addition, a noticeable difference between the shift calculated by the EBM when compared to that calculated by the SBM is observed, increasing the nanobeam dimensions due to the shear effect. This result confirms that the influence of shear should be considered and thus, the SBM is most suitable to investigate the adatom-nanobeam systemdue tothe change in the $\chi_b(\alpha,N).\chi_m(\alpha,N)/\chi_s(\alpha,N)$ value. The non-local SBM should be used for the suitable prediction of the dynamic vibration in lieu of the non-local EBM, which ignores the effects of shear stiffness. In addition, the network of periodic square holes makes the adatom-nanobeam system softer and changes the non-local shift versus the system thickness and mode number. This indicates the advantages of the perforated nanostructure toward the design of the adatom-nanobeam system with respect to the full nanostructure. Moreover, the change in the adatom density produces distinct behavior due to the competition between total bending and total mass. Therefore, this investigation provides a physical approach that maybe useful for the development of adatom sensing microdevices.

Acknowledgments

The authors thank the University of Franche-Comté for the "mobilités entrantes 2018" funding (Convention N°2018-0087), allowing fruitful collaboration.

References

[1] Y. Song, M. Kim, M. Seo, J. Yoon, A Complementary Dual-Contact MEMS Switch Using a “Zipping” Technique, Journal of Microelectromechanical Systems, 23 (2014), 710–718.
[2] A.M. Zenkour, A.E. Abouelregal, Vibration of FG nanobeams induced by sinusoidal pulse-heating via a non-local thermoelastic model, Acta Mechanica, 225 (2014), 3409–3421.
[3]B. Bakhadda, M.B. Bouiadjra, F. Bourada, A.A. Bousahla, A. Tounsi, S.R. Mahmoud, Dynamic and bending analysis of carbon nanotube-reinforced composite plates with elastic foundation, Wind and Structures, 27 (2018), 311–324.
[4]M. Ahouel, M.S.A. Houari, E.A.A. Bedia, A. Tounsi, Size-dependent mechanical behavior of functionally graded trigonometric shear deformable nanobeams including neutral surface position concept, Steel and Composite Structures, 20 (2016), 963–981.
[5]K. Bouafia, A. Kaci, M.S.A. Houari, A. Benzair, A. Tounsi, A non-local quasi-3D theory for bending and free flexural vibration behaviors of functionally graded nanobeams, Smart Structures and Systems, 19 (2017), 115–126.
[6]B. Karami,D. Shahsavari,M. Janghorban,A.Tounsi, Resonance behavior of functionally graded polymer composite nanoplates reinforced with grapheme nanoplatelets, International Journal of Mechanical Sciences, 156 (2019), 94–105.
[7] R. Ansari, F. Alisafaei, A. Alipour, E. Mahmoudinezhad, On the van der Waals interaction of carbon nanocones, Journal of Physics and Chemistry of Solids, 73 (2012), 751–756.
[8] M.-A. Salam, S. Sufian, Y. Lwin, Hydrogen adsorption study on mixed oxides using the densityfunctional theory, Journal of Physics and Chemistry of Solids, 74 (2013), 558–564.
[9] J.-Q. Zhang, S.-W. Yu, X.-Q. Feng, Theoretical analysis of resonance frequency change induced by adsorption, Journal of Physics D: Applied Physics, 41 (2008), 125306–?.
[10] J.-Q. Zhang, S.-W. Yu, X.-Q. Feng, G.-F. Wang, Theoretical analysis of adsorption-induced microcantilever bending, Journal of Applied Physics, 103 (2008), 093506–?.
[11] B. Gheshlaghi, S.M. Hasheminejad, Adsorption-induced resonance frequency shift in Timoshenko microbeams, Current Applied physics, 11 (2011), 1035–1041.
[12] G. Chen, T. Thundat, E. Wachter, R. Warmack, Adsorption-induced surface stress and its effects on resonance frequency of microcantilevers, Journal of Applied Physics, 77 (1995), 3618–3622.
[13] S. Cherian, T. Thundat, Determination of adsorption-induced variation in the spring constant of a microcantilever, Applied Physics Letters, 80 (2002), 2219–2221.
[14] M.F. Hagan, A. Majumdar, A.K. Chakraborty, Nanomechanical forces generated by surface grafted DNA, The Journal of Physical Chemistry B, 106 (2002), 10163–10173.
[15] D.F. Wang, T. Ono, M. Esashi, Thermal treatments and gas adsorption influences on nanomechanics of ultra-thin silicon resonators for ultimate sensing, Nanotechnology, 15 (2004), 1851–?.
[16] S. Kim, D. Lee, X. Liu, C. Van Neste, S. Jeon, T. Thundat, Molecular recognition using receptor-free nanomechanical infrared spectroscopy based on a quantum cascade laser, Scientific reports, 3 (2013), 1111–?.
[17] F. Huber, H. Lang, N. Backmann, D. Rimoldi, C. Gerber, Direct detection of a BRAF mutation in total RNA from melanoma cells using cantilever arrays, Nature nanotechnology, 8 (2013) 125–?.
[18] E. Sage, A. Brenac, T. Alava, R. Morel, C. Dupré, M.S. Hanay, M.L. Roukes, L. Duraffourg, C. Masselon, S. Hentz, Neutral particle mass spectrometry with nanomechanical systems, Nature communications, 6 (2015), 6482–?.
[19] C. Girardet, D. Vardanega, F. Picaud, Selective detection of chiral molecules by chiral single walled nanotubes, Chemical physics letters, 443 (2007), 113–117.
[20] D. Vardanega, F. Picaud, C. Girardet, Towards selective detection of chiral molecules using SWNT sensors, Surface Science, 601 (2007), 3818–3822.
[21] F. Picaud, G. Herlem, C. Girardet, Control of carbon nanotube handedness using a supramolecular chiral surface, The Journal of chemical physics, 135 (2011), 154703–?.
[22]R. Barretta,M. Čanadija,L. Feo,R. Luciano,F. M. d. Sciarra, Exact solutions of inflected functionally graded nanobeams in integral elasticity, Composites Part B: Engineering, 142 (2018), 273–286.
[23]R. Barretta, F. Fabbrocino, R. Luciano, F.M.d. Sciarra, Closed-form solutions in stress-driven two-phase integral elasticity for bending of functionally graded nanobeams, Physica E: Low-dimensional Systems and Nanostructures, 97 (2018), 13–30.
[24] S.S. Mirjavadi,B.M. Afshari,M.R. Barati,A.M.S. Hamouda, Transient response of porous FG nanoplates subjected to various pulse loads based on non-local stress-strain gradient theory, European Journal of Mechanics - A/Solids, 74 (2018),210–220.
[25]A. Apuzzo, R. Barretta, S.A. Faghidian, R. Luciano, F.M.d. Sciarra, Free vibrations of elastic beams by modified non-local strain gradient theory, International Journal of Engineering Science, 133 (2018), 99–108.
[26] A.G. Arani, V. Atabakhshian, A. Loghman, A. Shajari, S. Amir, Non-linear vibration of embedded SWBNNTs based on non-local Timoshenko beam theory using DQ method, Physica B: Condensed Matter, 407 (2012), 2549–2555.
[27] J. Wang, Y. Gao, M.-Y. Ng, Y.-C. Chang, Radial vibration of ultra-small nanoparticles with surface effects, Journal of Physics and Chemistry of Solids, 85 (2015), 287–292.
[28]Y. Mokhtar, H. Heireche, A.A. Bousahla, M.S.A. Houari, A. Tounsi, S.R. Mahmoud, A novel shear deformation theory for buckling analysis of single layer graphene sheet based on non-local elasticity theory, Smart Structures Systems, 21 (2018),397–405.
[29] R.C. Dixon, A.C. Eringen, A dynamical theory of polar elastic dielectricsI, International Journal of Engineering Science, 3 (1965), 359–377.
[30] M.R. Farajpour, A.R. Shahidi, A. Hadi, A. Farajpour, Influence of initial edge displacement on the non-linear vibration, electrical and magnetic instabilities of magneto-electro-elastic nanofilms, Mechanics of Advanced Materials and Structures, (2018), 1–13.
[31]A. Farajpour, A. Rastgoo,M.R. Farajpour, Non-linear buckling analysis of magneto-electro-elastic CNT-MT hybrid nanoshells based on the non-local continuum mechanics, Composite Structures, 180 (2017),179–191.
[32]C. Li,H. Guo,X. Tian,T. He, Size-dependent thermo-electromechanical responses analysis of multi-layered piezoelectric nanoplates for vibration control, Composite Structures, 225 (2019),111112–?.
[33]M. Kamali,M. Shamsi,A.R. Saidi, Surface effect on buckling of microtubules in living cells using first-order shear deformation shell theory and standard linear solid model, Mechanics Research Communications, 92 (2018),111–117.
[34]M.R. Farajpour, A.R. Shahidi, A. Farajpour, Frequency behavior of ultrasmall sensors using vibrating SMA nanowire-reinforced sheets under a non-uniform biaxial preload, Materials Research Express, 6 (2019),065047–?.
[35]C. Li, H. Guo, X. Tian, T. He, Non-local diffusion-elasticity based on non-local mass transfer and non-local elasticity and its application in shock-induced responses analysis, Mechanics of Advanced Materials and Structures, (2019),1–12.

[36]M.R. Farajpour, A. R. Shahidi, F.T. Nasab, A. Farajpour, Vibration of initially stressed carbon nanotubes under magneto-thermal environment for nanoparticle delivery via higher-order non-local strain gradient theory, European Physical Journal Plus, 133 (2018), 219–?.
[37]A. Mouffoki, E.A.A. Bedia, M.S.A. Houari, A. Tounsi, S.R. Mahmoud, Vibration analysis of non-local advanced nanobeams in hygro-thermal environment using a new two-unknown trigonometric shear deformation beam theory, Smart Structures Systems , 20 (2017),369–383.
[38]B. Karami, M. Janghorban, A. Tounsi, Non-local strain gradient 3D elasticity theory for anisotropic spherical nanoparticles, Steel and Composite Structures, 27 (2018),201–216.
[39]C. Li,L. Yao, W. Chen,S. Li, Comments on non-local effects in nano-cantilever beams, International Journal of Engineering Science, 87 (2018), 47–57.
[40]N. Challamel, C.M. Wang, The small length scale effect for a non-local cantilever beam: Aparadox solved, Nanotechnology, 19 (2008),345703–?.
[41] H.-T. Thai, A non-local beam theory for bending, buckling, and vibration of nanobeams, International Journal of Engineering Science, 52 (2012), 56–64.
[42]R. Talebitooti, S. O. Rezazadeh, A. Amiri, Comprehensive semi-analytical vibration analysis of rotating tapered AFG nanobeams based on non-local elasticity theory considering various boundary conditions via differential transformation method, Composites Part B: Engineering, 160 (2019), 412–435.
[43]S. H. Hashemi, H. B. Khaniki, Dynamic response of multiple nanobeam system under a moving nanoparticle, Alexandria Engineering Journal, 57 (2018), 343–356.
[44] R. Firouz-Abadi, M. Fotouhi, H. Haddadpour, Dynamical parametric instability of carbon nanotubes under axial harmonic excitation by non-local continuum theory, Journal of Physics and Chemistry of Solids, 95 (2016), 19–23.
[45] K. Kiani, Postbuckling scrutiny of highly deformable nanobeams: A novel exact non-local surface energy-based model, Journal of Physics and Chemistry of Solids, 110 (2017), 327–343.
[46]K. Ghorbani, K. Mohammadi, A. Rajabpour, M. Ghadiri, Surface and size-dependent effects on the free vibration analysis of cylindrical shell based on Gurtin-Murdoch and non-local strain gradienttheories, Journal of Physics and Chemistry of Solids, 129 (2019), 140–150.
[47] S. Hosseini-Hashemi, R. Nazemnezhad, H. Rokni, Non-local non-linear free vibration of nanobeams with surface effects, European Journal of Mechanics-A/Solids, 52 (2015), 44–53.
[48] X.-j. Xu, Z.-c. Deng, Surface effects of adsorption-induced resonance analysis on micro/nanobeams via non-local elasticity, Applied Mathematics and Mechanics, 34 (2013), 37–44.
[49] A. Ghorbanpourarani, M. Mohammadimehr, A. Arefmanesh, A. Ghasemi, Transverse vibration of short carbon nanotubes using cylindrical shell and beam models, Proceedings of the Institution of Mechanical Engineers, Part C: Journal of Mechanical Engineering Science, 224 (2010), 745–756.
[50] H. Bourouina, R. Yahiaoui, R. Kerid, M.E.A. Benamar, F. Brioua, Mathematical model for the adsorption-induced non-local frequency shift in adatoms-nanobeam system, Physica B: Condensed Matter, 520 (2017), 128–138.
[51] K. Ghoumid, I. Elhechmi, S. Mekaoui, C. Pieralli, T. Gharbi, Analysis of optical filtering in waveguides with a high index modulation using the extended coupled mode theory by hybridization of a matrix method, Optics Communications, 289 (2013), 85–91.
[52]S. Hedayatrasa, K. Abhary, M. Uddin, C. T. Ng, Optimum design of phononic crystal perforated plate structures for widest bandgap of fundamental guided wave modes and maximized in-plane stiffness, Journal of the Mechanics and Physics of Solids, 89 (2016), 31–58.
[53] J. Liu, L. Li, B. Xia, X. Man, Fractal labyrinthine acoustic metamaterial in planar lattices, International Journal of Solids and Structures, 132 (2018), 20–30.
[54] J. Chen, B. Xia, J. Liu, A sparse polynomial surrogate model for phononic crystals with uncertain parameters, Computer Methods in Applied Mechanics and Engineering, 339 (2018), 681–703.
[55] R. Miura, S. Imamura, R. Ohta, A. Ishii, X. Liu, T. Shimada, S. Iwamoto, Y. Arakawa, Y. Kato, Ultralow mode-volume photonic crystal nanobeam cavities for high-efficiency coupling to individual carbon nanotube emitters, Nature communications, 5 (2014), 5580–?.
[56] T. Fras, C.C Roth, D. Mohr, Fracture of high-strength armor steel under impact loading, Journal of Vacuum Science & Technology B: Microelectronics and Nanometer Structures Processing, Measurement, and Phenomena, 111 (2018), 147–167.
[57] Orun, Arif E, A. Guler, Effect of hole reinforcement on the buckling behaviour of thin-walled beams subjected to combined loading, Thin-Walled Structures, 118 (2017), 12–22.
[58] P. Candelas, J. M. Fuster, S. Pérez-López, A. Uris, C. Rubio, Observation of ultrasonic Talbot effect in perforated plates, Ultrasonics, 94 (2019) 281–284.
[59] L. Luschi, F. Pieri, An analytical model for the determination of resonance frequencies of perforated beams, Journal of Micromechanics and Microengineering, 24 (2014), 055004–?.
[60] M. Eltaher, A. Kabeel, K. Almitani, A. Abdraboh, Static bending and buckling of perforated non-local size-dependent nanobeams, Microsystem Technologies, 24 (2018), 4881–4893.
[61] H. Bourouina, R. Yahiaoui, A. Sahar, M.E.A. Benamar, Analytical modeling for the determination of non-local resonance frequencies of perforated nanobeams subjected to temperature-induced loads, Physica E: Low-dimensional Systems and Nanostructures, 75 (2016), 163–168.
[62] R. Kerid, H. Bourouina, R. Yahiaoui, M. Bounekhla, A. Aissat, Magnetic field effect on non-local resonance frequencies of structure-based filter with periodic square holes network, Physica E: Low-dimensional Systems and Nanostructures, 105 (2019), 83–89.
[63] G.-F. Wang, X.-Q. Feng, Effects of surface elasticity and residual surface tension on the natural frequency of microbeams, Applied Physics Letters, 90 (2007), 231904–?.
[64] R. Gabbai, H. Benaroya, An overview of modeling and experiments of vortex-induced vibration of circular cylinders, Journal of Sound and vibration, 282 (2005), 575–616.
[65] X.-F. Li, K.Y. Lee, Effect of horizontal reaction force on the deflection of short simply supported beams under transverse loadings, International Journal of Mechanical Sciences, 99 (2015), 121–129.
[66] M. Aydogdu, V. Taskin, Free vibration analysis of functionally graded beams with simply supported edges, Materials & design, 28 (2007) 1651–1656.
[67] A. Benjeddou, J.-F. Deü, S. Letombe, Free vibrations of simply-supported piezoelectric adaptive plates: an exact sandwich formulation, Thin-walled structures, 40 (2002), 573–593.
[68] A.G. Arani, M. Roudbari, Surface stress, initial stress and Knudsen-dependent flow velocity effects on the electro-thermo non-local wave propagation of SWBNNTs, Physica B: Condensed Matter, 452 (2014), 159–165.
[69] S. Kumar, R. Pratap, Partitioning design space for linear tuning of natural frequencies in planar dynamic MEMS structures, Sensors and Actuators A: Physical, 125 (2006), 304–312.

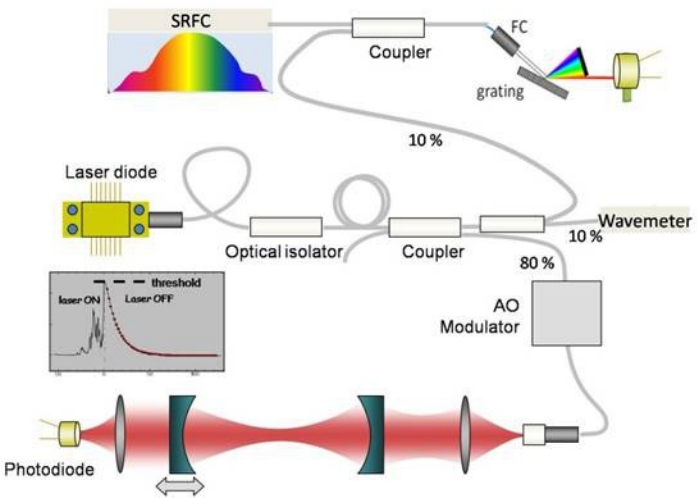
SRFC
Coupler
FC
grating
10 %
Laser diode
Optical isolator
Coupler
Wavemeter
10 %
80 %
threshold
laser ON
Laser OFF
AO
Modulator
Photodiode

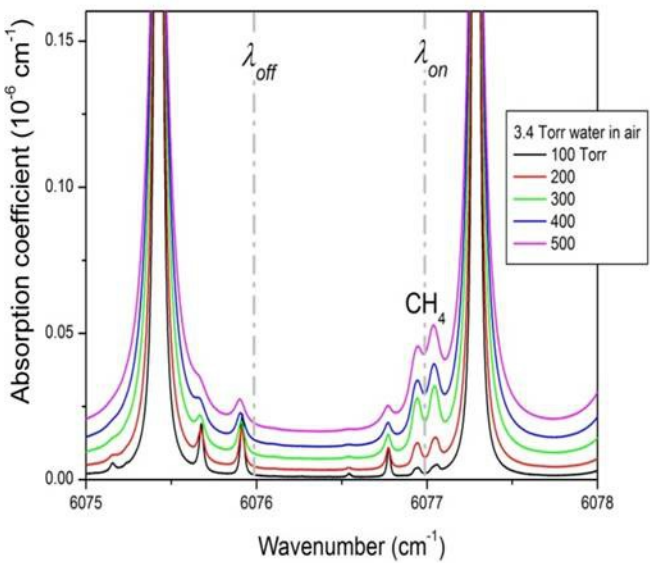
Absorption coefficient (10^{-6} cm^{-1})
Wavenumber (cm^{-1})
λ_{off}
λ_{on}
CH_4
3.4 Torr water in air
100 Torr
200
300
400
500
0.00
0.05
0.10
0.15
6075
6076
6077
6078

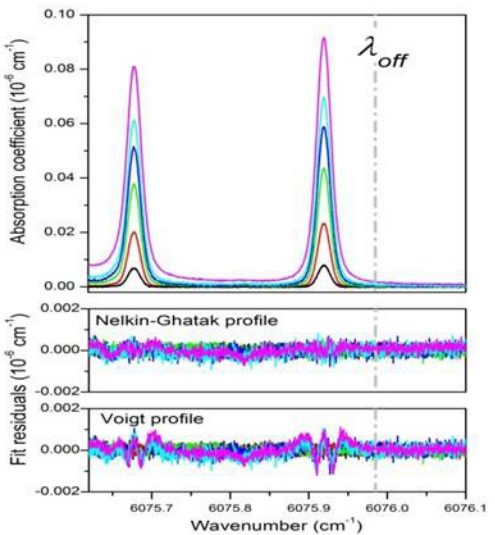
Absorption coefficient (10^{-6} cm^{-1})
λ_{off}
Nelkin-Ghatak profile
Voigt profile
Fit residuals (10^{-6} cm^{-1})
Wavenumber (cm^{-1})
6075.7
6075.8
6075.9
6076.0
6076.1